Asian Journal of Chemistry; Vol. 26, No. 1 (2014), 127-131

ASIAN JOURNAL OF CHEMISTRY

http://dx.doi.org/10.14233/ajchem.2014.15348

Synthesis and Characterization of 3D CuO Hierarchical Structure by Nanoplates Two-Step Self-Assembly

XIAOYAN LIU[1,*,†], HONGMEI ZANG[1,†], JUE SONG[1], JIHUI TANG[1] and YITAI QIAN[2]

[1]College of Pharmacy, Anhui Medical University, 81 Meishan Road, Hefei 230032, Anhui Province, P.R. China
[2]Hefei National Laboratory for Physical Science at Microscale and Department of Chemistry, University of Science and Technology of China, Hefei 230026, Anhui Province, P.R. China

*Corresponding author: Email: liuxy8@mail.ustc.edu.cn; liuxyhrz@163.com
†These authors have equal contribution to this work.

Received: 18 February 2013; *Accepted*: 17 May 2013; *Published online*: 26 December 2013; AJC-14487

A simple hydrothermal route was developed to synthesize CuO three-dimensional (3 D) hierarchical microspheres with average diameter of about 3 μm. The formation of CuO hierarchical microspheres involves in two stages: tiny nanoplates attached side by side first constitute 2 D nanosheets *via* an orientation attachment growth mode. Then as-formed sheets assemble orderly and align radially from the center through a layer-by-layer growth style so as to form well-fined microspheres with a multilayered structure. A systematic investigation was carried out to understand the factors influencing the CuO morphology. The quantity of PEG played crucial roles in the formation of CuO hierarchical structures. The possible growth mechanism was identified to explain the formation of CuO architectures herein.

Keywords: CuO, Hierarchical structure, Microspheres, Orientation aggregation.

INTRODUCTION

It is well known that physical properties of nanomaterials are usually closely related to size, shape and dimensionality. Low-dimensional nanostructures, including nanodots, nanorods and nanosheets, have stimulated intensive interest over the past few years due to their potential applications in nanoscale devices based on their special properties in mesoscopic physics compared with those of the corresponding bulk crystals[1-2]. Recently, with the realization of technologically useful low-dimensional nanostructure-based materials which depend not only on the quality of the nanocrystals (*e.g.*, size and dimensionality) but also on their spatial orientation and arrangement[3], research is expanding into the assembly of low-dimensional nanoscale building blocks into two- and three-dimensional ordered superstructures or complex functional architectures, which is a crucial step toward the realization of functional nanosystems[4-7]. To obtain well-arranged low-dimensional nanostructures, capping reagents are usually introduced to reduce the activity of nanobuilding blocks so as to promote or tune the ordered self-assembly.

As an important transition metal oxide with a narrow band gap (Eg = 1.2 eV), CuO, forms the basis of several high temperature superconductors and giant magnetoresistance materials[8]. It is also a promising material for facbricating solar cells[9] and lithium ion battery[10], owing to its photoconductive and photochemical properties. Therefore, the synthesis and assembly of CuO nanostructures with different forms of controlled nanostructures have both fundamental and practical importance and have attracted considerable attention in recent years. Up to date, low-dimensional CuO nanostructures such as nanowires[11], nanorods[12-15], nanoribbons/nanobelts[16-19], nanotubes[20] and nanoplates[21,22] have been largely prepared through different routes. In particular, recent research indicates that 2 D and 3 D ordered superstructures of CuO nanomaterials have been widely focused. For example, Qian *et al.*[23] have fabricated well-aligned CuO nanoplatelet arrays. Yu *et al.*[24] have prepared peanut-shaped nanoribbon bundle superstructures through thermal decomposition of malachite precursor with similar morphology. Zeng's group[25] has synthesized dandelion-like CuO hollow microspheres made up of nanoribbons through hydrothermal method. Although great progresses have been made in the systhesis of CuO architectures, however, fabrication of CuO hierarchical microspheres using univalent copper salt CuCl as reagent *via* an oxidation process has been rarely reported. Generally, CuO were obtained through employing Cu^{2+} -contained precursors as reagent in alkaline medium *via* the heat treatment, where no oxidation-redox process was involved. In this paper, we present a simple hydrothermal route to synthesize CuO hierarchical microspheres applying CuCl

as copper source *via* an oxidation process in the presence of PEG as surfactant. The growth mechanism of CuO hierarchical microspheres were investigated in detail. Our results enrich the hierarchical CuO architecture family.

EXPERIMENTAL

All the reagents used in the experiment were analytically pure, purchased from Shanghai Chemical Reagent Company and used without further purification.

In all the synthesis procedures, the amount of CuCl was kept 1 mmol constant. In a typical procedure to prepare CuO hierarchical microspheres, 0.6 g PEG20000 was dissolved in 40 mL distilled water with continuous stirring. Then, 1 mmol cuprous chloride (CuCl) dissolved in 5 mL aqueous ammonia was added dropwise into the above solution. After being stirred for 10 min, the mixtures were transferred into a Teflon-lined stainless autoclave (60 mL capacity). The autoclave was sealed and maintained at 120 °C for 10 h. The system was then cooled to ambient temperature naturally. The final product was collected and washed with distilled water and absolute alcohol several times, vacuum-dried and kept for further characterization. The resulting precipitate was retrieved by centrifugation, washed several times with distilled water and absolute alcohol to remove impurities and then dried in a vacuum at 50 °C for 4 h.

Characterization of samples: X-ray powder diffraction (XRD) patterns of the products were recorded on a Japanese Rigaku D/max-γA X-ray diffractometer equipped with graphite-monochromatized CuK_{α_1} radiation (λ = 1.54178 Å). X-ray photoelectron spectroscopy (XPS) was carried out on a VGESCALAB MKL X-ray photoelectron spectrometer, using nonmonochromatized MgKα X-ray as the excitation source. The field emission scanning electron microscope (FESEM) images of the products were recorded on a JEOL JSM-6300F microscope. The transmission electron microscope (TEM) images were taken on a Hitachi (Tokyo) H-800 transmission electron microscope at an accelerating voltage of 200 kV. The selected area electron diffraction (SAED) patterns were recorded on a JEOL 2010 microscope.

RESULTS AND DISCUSSION

Morphology and structure characterization of CuO hierarchical microspheres: The typical XRD pattern of the product is shown in Fig. 1. The obtained product displays the characteristic XRD peaks corresponding to the monoclinic CuO (space group C2/c) [JCPDS Card No. 80-1268]. No characteristic XRD peaks arising from other crystalline impurities are detected, exhibiting the high purity of as-prepared CuO nanostructures under the experimental conditions.

The samples obtained are further examined by infrared analysis (Fig. 2). According to the group theoretical theory and the fact that CuO belongs to the C^6_{2h} space group with two molecules per primitive cell, one can contribute to the zone center normal modes:

$$\Gamma = 4\,Au + 5\,Bu + Ag + 2\,Bg$$

There are six infrared active modes (3 Au + 3 Bu), three acoustic modes (Au + 2 Bu) and three Raman active modes (Ag + 2 Bg). As shown in Fig. 2, for every CuO sample there

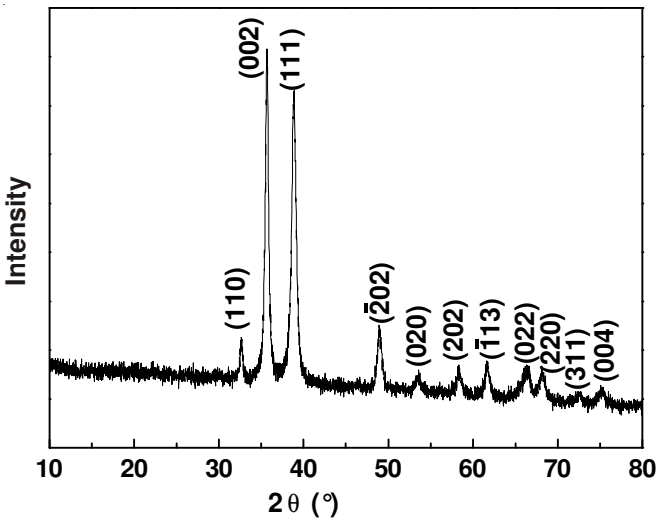

Fig. 1. XRD pattern of CuO hierarchical microspheres

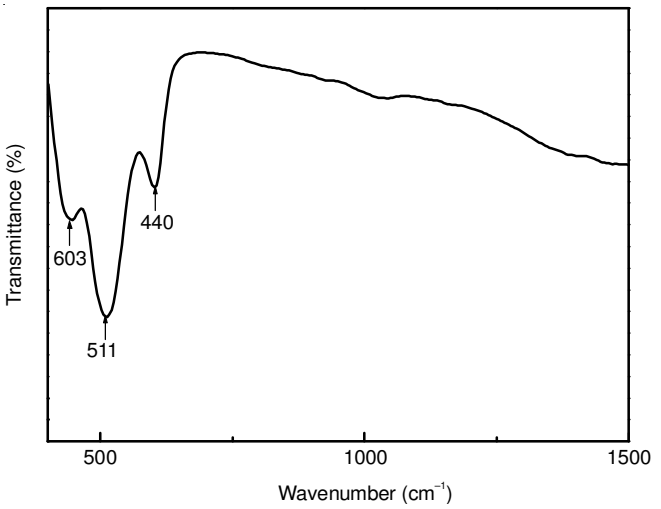

Fig. 2. Infrared spectrum of CuO hierarchical microspheres

are all three infrared peaks observed at 440, 511 and 602 cm^{-1}, which are assigned to the Au mode, Bu mode and another Bu mode, respectively. The high-frequency mode at 602 cm^{-1} may be a Cu-O stretching along the $[\bar{1}01]$ direction and the mode at 511 cm^{-1} may be Cu-O stretching along [101] direction. Compared with the data reported[19], there exists some slight difference. It may be resulted from the variation in sample types, temperatures and broadness of the spectrum. Moreover, no other infrared active modes can be observed (such as Cu_2O, appearing at 615 cm^{-1}). Consequently, IR analysis also confirms that the as-obtained products are pure-phase CuO with monoclinic structure.

Fig. 3 shows typical FESEM images of the product. As shown in Fig. 3a, the product consists of a number of uniform spheres with average diameter of about 3 μm. An enlarged FESEM image indicates that each microsphere is composed of a lot of stacked two-dimensional (2D) nanosheets with the thickness of 40 nm (Fig. 3b). The image of Fig. 3c well reveals the intact detail of a single sphere, which further shows that a single sphere consists of a number of nanosheets. These nanosheets arrange radially from the center and form a multilayered structure. From the inset in Fig. 3c, we can further find that each layer/sheet is made up of numerous tiny nanopaltes

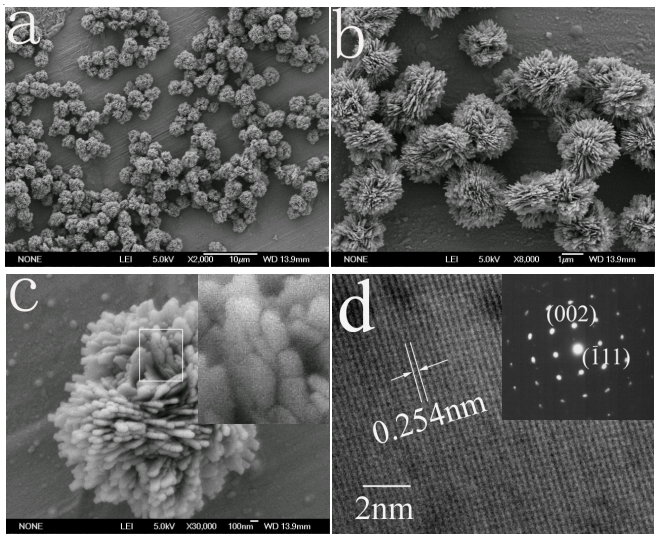

Fig. 3. (a-c) FESEM images, (d) HRTEM image of CuO hierarchical microspheres. The inset in d shows the SAED pattern

(inset of Fig. 3c). These tiny nanoplates are attached side by side into an integrated sheet, which perhaps indicates an orientation attachment growth mode and is highly similar to the formation process of Bi_2WO_6 microspheres[26]. On the basis of the above results, the formation of microspheres probably involves in two stages: tiny nanoplates first constitute 2 D nanosheets *via* an orientation attachment growth mode. Then as-formed sheets assemble orderly and align radially from the center through a layer-by-layer growth style so as to form well-fined microspheres with a multilayered structure. Obviously, the as-prepared micorspheres can be generally classified as hierarchical structures. It is worth mentioning that these hierarchical microspheres are adequately stable so that they can not be destroyed into dispersed nanoplates even after long time ultrasonication, which may be attributed to strong attachment ability among tiny nanoplates and assembly interaction among 2 D nanosheets. The microstructure of as-obtained CuO product is further investigated by HRTEM and SAED microscopy, which were obtained from the edge of a nanosheet. The HRTEM image exhibits that the regular spacing of the clear lattice planes is ca. 0.254 nm, which correspond well to (002) planes of monoclinic-phase CuO. The SAED pattern can be indexed to be the [001] zone axis of monoclinic phase CuO. These pattern spots are consistent with XRD results and demonstrate that the CuO nanoplate has a single-crystalline nature.

Effects of the reaction conditions on CuO hierarchical architectures: In this strategy, we explored the influencing factors and optimized the reaction conditions. It is notable that many factors play important roles to control the morphologies of CuO crystals, such as the reaction temperature, the concentration of PEG and the reaction time. These factors will be studied using the following processes. It is found that CuO spherical architectures assembled of nanoflakes can obtained in a wide temperature range from 90-180 °C. As the reaction temperature increased, the size of CuO nanoflakes slightly increased, while the morphology of product did not change remarkably, *i.e.*, the temperature exerted a role on the size instead of morphology. Therefore, in present work, all experiments were carried out at 120 °C which was kept constant in order to discuss the effects of other conditions.

It is found that the concentration of PEG remarkably affects the morphologies of CuO. As shown in Figs. 3 and 4, various CuO nanoarchitectures were obtained through simply regulating the amounts of PEG from 0 g to 0.3 g and 0.6 g to 1 g and keeping the other conditions unchanged, which is also illuminated in Fig. 5. When PEG was absent, only irregular and dispersed nanoplates were obtained (Fig. 4a, b) instead of assembly of nanoplates. From the TEM image of Fig. 4b, these nanoplates aggregated together optionally. With the increase of PEG to 0.3 g keeping the other conditions unchanged, 2 D leaves-like nanosheets assembled by smaller nanoplates were gained (Figs. 4c, d). The TEM image of Fig. 4d well depicts nanoleaves-like shape. In the presence of 0.3 g PEG, CuO nanoplates already assembled into 2 D nanoleaves-like morphology instead of absolutely irregular nanoplates. When the amount of PEG reached to 0.6 g, hierarchical microspheres were acquired as shown in Fig. 3. As the above-mentioned discussion, these microspheres were constructed by many 2 D sheets, which were densely packed and formed a multilayered structure. It was further found that each sheet was made up of numerous tiny nanoplates. Further increasing the amount of PEG to 1 g (Figs. 4e, f), similarly, hierarchical microspheres assembled by nanosheets were prepared. To mention, comparing the morphologies of CuO products in the presence of 0.6 g (Fig. 3) with 1 g PEG (Figs. 4e, f), both well-defined hierarchical microspheres were obtained. However, the diversity is in that in the product with the addition of 1 g PEG (Fig. 4f)

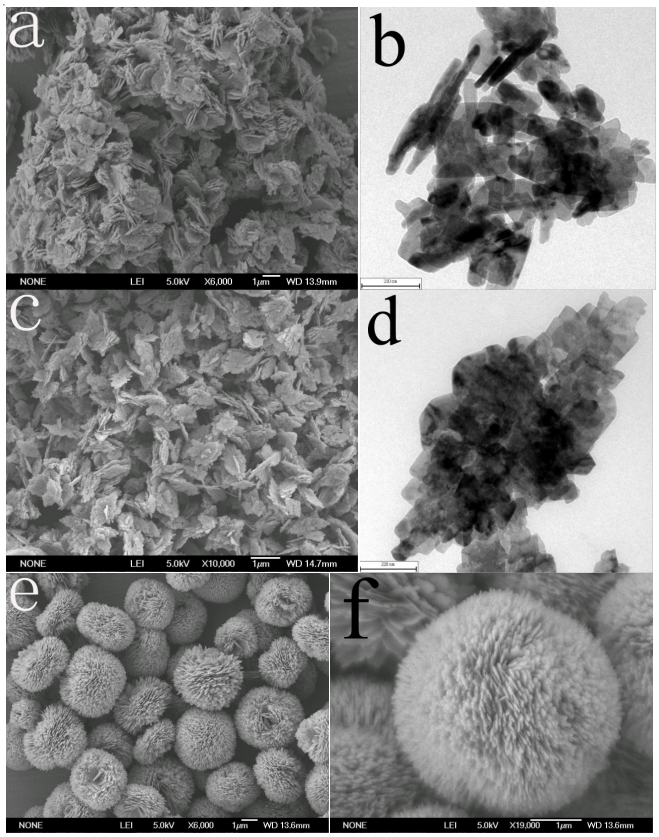

Fig. 4. FESEM and TEM images of CuO nanostructures prepared in the presence of (a) and (b) 0 g PEG, (c) and (d) 0.3 g PEG, (e) and (f) 1 g PEG

nanosheets arranged more densely and assembled compactly one another. Careful investigation for the product with the addition of 0.6 g PEG (Fig. 3c) reveals that layer-by-layer stack among sheets in the Fig. 3c is relatively sparse and incompact and the gaps of layers are clearly eyeable. Therefore, on the basis of the above discussion, CuO morphologies are incisively influenced by the amounts of PEG. Generally, PEG acts not only as the shape-controlling agent but also as the stabilizing agent. In our synthesis conditions, PEG plays a vital role in the formation of hierarchical CuO architectures.

Growth mechanism of CuO 3 D architectures: To substantially understand the growth process of hierarchical CuO spherical architecture, time-dependent experiments were conducted. The products prepared at various stages were followed by TEM images. Fig. 5 shows TEM images of the intermediate samples obtained at 10, 20 and 60 min. As shown in Fig. 5a, assembled nanoplates aggregates initially formed, which were the rudiment of CuO spherical architecteures. By reason of these nanoplates filling up incompactly, the cavity in the center of the aggregates is clearly observed. With the reaction time prolonged (Figs. 5b, c), some underdeveloped aggregates which stacked loosely accompanying primary well-developed spherical architectures gradually formed and the aggregates markedly stacked more compactly. As reaction time further prolonging (Fig. 5d), mainly well-defined spherical architectures formed at last. It is found that even prolonging reaction time above 1 h even longer than 10 h, both morphology and size are similar to the sample at 1 h.

Based on the FESEM and TEM observations, it is concluded that layer-by-layer growth resulted in the formation of CuO hierarchical structures. The detailed growth process of the products may be described as follows: Initially, CuCl dissolved in aqueous ammonia and formed $[Cu(NH_3)_2]^+$ complex. Then $[Cu(NH_3)_2]^+$ complex was oxidated by O_2 obturated in the autoclave so as to become $[Cu(NH_3)_4]^{2+}$ complex. As-formed $[Cu(NH_3)_4]^{2+}$ complex immediately hydrolyzed into $Cu(OH)_2$. Instantly, CuO nucleus were formed *via* a rapid dehydration process of $Cu(OH)_2$ with the hydrothermal treatment. Correlative reaction equations are as the following:

$$4\,[Cu(NH_3)_2]^+ + 8\,NH_3{\cdot}H_2O + O_2 \rightarrow 4\,[Cu(NH_3)_4]^{2+} + 4\,OH^- + 6\,H_2O \quad (1)$$

$$[Cu(NH_3)_4]^{2+} + 2\,H_2O \rightarrow Cu(OH)_2 + 2NH_4^+ + 2\,NH_3 \quad (2)$$

$$Cu(OH)_2 \rightarrow CuO + H_2O \quad (3)$$

It is well known that CuO nanoplates are easy to form because of the intrinsic structural feature. Therefore, we believe that the formation of initial CuO nucleus was tiny nanoplates. With the nucleus increasing until saturation concentration, the growth process occurs and CuO nanoplates will aggregate. In the present case, it is possible that the selective absorption of PEG on certain crystallographic planes. When no protective agent was present, CuO nanoplates underwent a random aggregation (Figs. 4a, b), which resulted in the formation of irregular and dispersed nanoplates. When 0.3 g PEG was introduced, owing to the selective absorption of PEG on certain CuO crystallographic planes, initially formed nanoplates assembled in an edge-to-edge way into a leaves-like sheet (Figs. 4c, d). With the increase of PEG to 0.6 g, *in situ* nanosheets tended to stack *via* a layer-by-layer growth style from a center, which will finally formed microspheres with multilayered structures. This process could further reduce the surface energy of nanosheets. Further increased PEG to 1 g, the correlative evolved process is similar, but the layers are denser and the stacks are thicker, which results in more delicate microspheres (Figs. 4e, f).

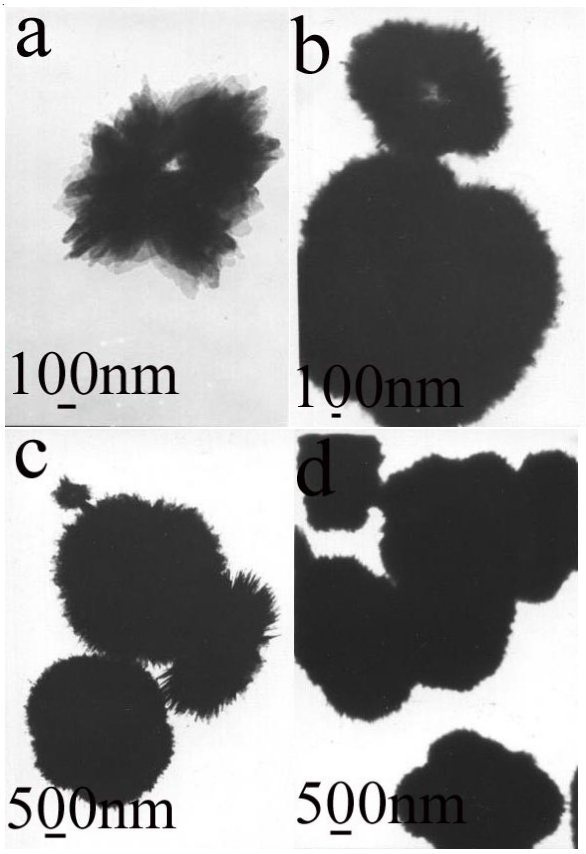

Fig. 5. TEM images of pricky CuO microspheres at 120 °C for different reaction time: (a) 10 min, (b) and (c) 20 min, (d) 1 h

Conclusion

A simple hydrothermal route has been developed to synthesize CuO 3D hierarchical microspheres with average diameter of about 3 μm using CuCl as the copper source and PEG as the morphology-directing agent in aqueous ammonia medium. A systematic investigation has been carried out to understand the factors influencing the CuO morphology. The quantity of PEG markedly influenced the morphologies of CuO architectures. The microspheres were constructed from two-dimensional (2 D) nanosheets with average thickness of about 40 nm *via* a layer-by-layer growth style. These nanosheets arrange radially from the center and form a well-fined microsphere with a multilayered structure. Interestingly, the nanosheets were further composed of tiny nanoplates through orientation attachment.

ACKNOWLEDGEMENTS

This study was supported by Grants for Scientific Research of BSKY (No. XJ200902) from Anhui Medical University and the School Scientific Research Funds of Anhui Medical University (No. 2010xkj008)

REFERENCES

1. Y. Cui, Q.Q. Wei, H.K. Park and C.M. Lieber, *Science*, **293**, 1289 (2001).
2. G. Schmid, *Chem. Rew*., **92**, 1709 (1992).
3. M.H. Huang, S. Mao, H. Feick, H.Q. Yan, Y.Y. Wu, H. Kind, E. Weber, R. Russo and P.D. Yang, *Science*, **292**, 1897 (2001).
4. L. Manna, E.C. Scher and A.P. Alivisatos, *J. Am. Chem. Soc*., **122**, 12700 (2000).
5. S.M. Lee, Y.W. Jun, S.N. Cho and J. Cheon, *J. Am. Chem. Soc*., **124**, 11244 (2002).
6. Y. Wu, H. Yan, M. Huang, B. Messer, J.H. Song and P.D. Yang, *Chem. Eur. J*., **8**, 1261 (2002).
7. H.T. Shi, L.M. Qi, J.M. Ma, H.M. Cheng and B.Y. Zhu, *Adv. Mater*., **15**, 1647 (2003).
8. (a) A.O. Musa, T. Akomolafe and M.J. Carter, *Sol. Energy Mater. Sol. Cells*, **51**, 305 (1998); (b) M.K. Wu, J.R. Ashburn, C.J. Torng, P.H. Hor, R.L. Meng, L. Gao, Z.J. Huang, Y.Q. Wang and C.W. Chu, *Phys. Rev. Lett*., **58**, 908 (1987); (c) X.G. Zheng, C.N. Xu, Y. Tomokiyo, E. Tanaka, H. Yamada and Y. Soejima, *Phys. Rev. Lett*., **85**, 5170 (2000); (d) D. Prabhakaran, C. Subramanian, S. Balakumar and P. Ramasamy, *Physica C*, **319**, 99 (1999); (e) K. Borgohain and S. Mahamuni, *J. Mater. Res*., **17**, 1220 (2002).
9. (a) T. Maruyama, *Sol. Energy Mater. Sol. Cells*, **56**, 85 (1998); (b) A.E. Rakhshni, *Solid State Electron*., **29**, 7 (1986).
10. (a) F. Lanza, R. Feduzi and J. Fuger, *J. Mater. Res*., **5**, 1739 (1990); (b) X.P. Gao, J.L. Bao, G.L. Pan, H.Y. Zhu, P.X. Huang, F. Wu and D.Y. Song, *J. Phys. Chem.*, B **108**, 5547 (2004).
11. X.C. Jiang, T. Herricks and Y.N. Xia, *Nano Lett*., **2**, 1333 (2002).
12. Q. Liu, Y.Y. Liang, H.J. Liu, J.M. Hong and Z. Xu, *Mater. Chem. Phys*., **98**, 519 (2006).
13. W.Z. Wang, Y.J. Zhan and G.H. Wang, *Chem. Commun.*, 727 (2001).
14. C.K. Xu, Y.K. Liu, G.D. Xu and G.H. Wang, *Mater. Res. Bull*., **37**, 2365 (2002).
15. L.L. Wang, H.X. Gong, C.H. Wang, D.K. Wang, K.B. Tang and Y.T. Qian, *Nanoscale*, **4**, 6850 (2012)
16. H.W. Hou, Y. Xie and Q. Li, *Cryst. Growth Des*., **5**, 201 (2005).
17. X.G. Wen, W.X. Zhang and S.H. Yang, *Langmuir*, **19**, 5898 (2003).
18. X.Y. Song, H.Y. Yu and S.X. Sun, *J. Colloid Interf. Sci*., **289**, 588 (2005).
19. X.J. Zhang, G.F. Wang, X.M. Liu and H.Q. Wu, *Mater. Chem. Phys*., **112**, 726 (2008).
20. M.H. Cao, C.W. Hu, Y.H. Wang, Y.H. Guo, C.X. Guo and E.B. Wang, *Chem. Commun.*, 1884 (2003).
21. F. Li, X.Q. Liu, Q. Zhang, T. Kong and H. Jin, *Cryst. Res. Technol*., **47**, 1140 (2012).
22. K.B. Zhou, R.P. Wang, B.Q. Xu and Y.D. Li, *Nanotechnology*, **17**, 3939 (2006).
23. G.F. Zou, H. Li, D.W. Zhang, K. Xiong, C. Dong and Y.T. Qian, *J. Phys. Chem. B*, **110**, 1632 (2006).
24. L.Z. Zhang, J.C. Yu, A.W. Xu, Q. Li, K.W. Kwong and S.H. Yu, *J. Cryst. Growth*, **266**, 545 (2004).
25. B. Liu and H.C. Zeng, *J. Am. Chem. Soc*., **126**, 8124 (2004).
26. Y.Y. Li, J.P. Liu, X.T. Huang and G.Y. Li, *Cryst. Growth Des.*, **7**, 1350 (2007).